and B. C. H. Steele, *ibid.*, **7,** 81 (1982); g, M. Stainer, L. C. Hardy, D. H. Whitmore, and D. F. Shriver, *This Journal,* **131,** 784 (1984); h, J. E. Weston and B. C. H. Steele, *Solid State Ionics,* **2,** 347 (1981); i, P. R. Sorensen and T. Jacobsen, *Electrochim. Acta,* **27,** 1671 (1982); j, B. L. Papke, M. A. Ratner, and D. F. Shriver, *This Journal,* **129,** 1694 (1982); k, B. L. Papke, M. A. Ratner, and D. F. Shriver, *ibid.*, 1484.
8. a, R. A. Reed, L. Geng, and R. W. Murray, *J. Electroanal. Soc.*, **208,** 185 (1986); b, L. Geng, R. A. Reed, M. L. Longmire, and R. W. Murray, *J. Phys. Chem.*, **91,** 2908 (1987); c, A. Bettelheim, R. A. Reed, N. H. Hendricks, J. P. Collman, and R. W. Murray, *J. Electroanal. Chem.*, **238,** 259 (1988); d, L. Geng, M. Longmire, R. A. Reed, J. F. Parcher, C. J. Barbour, and R. W. Murray, *Chem. Mater.*, **1,** 58 (1989); e, L. Geng, R. A. Reed, M.-H. Kim, T. Wooster, B. N. Oliver, J. Egekeze, R. Kennedy, J. W. Jorgenson, J. F. Parcher, R. W. Murray, *J. Am. Chem. Soc.*, **111,** 1614 (1989).
9. P. M. Blonsky, Ph.D. Thesis, Northwestern University, Evanston, IL (1986).
10. H. R. Allcock, P. E. Austin, T. X. Neeman, J. T. Sisko, P. M. Blonsky, and D. F. Shriver, *Macromolecules,* **19,** 1508 (1986).
11. B. P. Sullivan, D. J. Salmon, and T. J. Meyer, *Inorg. Chem.*, **17,** 3334 (1978).
12. C. S. Fuller, *Chem. Rev.*, **26,** 143 (1940).
13. R. Spindler and D. F. Shriver, *Macromolecules,* **21,** 648 (1988).
14. a, H. M. Koepp, H. Wendt, and H. Stretlow, *Z. Elektrochem.*, **64,** 483 (1960); b, C. A. Gagné and G. C. Lisensky, *Inorg. Chem.*, **19,** 2854 (1980).
15. M. B. Armand, M. J. Duclot, and P. Rigaud, *Solid State Ionics,* **3/4,** 429 (1981).
16. M. B. Armand, in "Lithium Nonaqueous Battery Electrochemistry," E. B. Yeager, B. Schomm, Jr., G. Blomgren, D. R. Blankenship, V. Leger, and J. Akridge, Editors, p. 261, The Electrochemical Society Softbound Proceedings Series, Pennington, NJ (1980).
17. C. A. C. Sequeira, J. M. North, and A. Hooper, *Solid State Ionics,* **13,** 175 (1984).
18. D. N. Palmer, J. E. Brule, M. Grayson, J. K. Alexander, and J. M. O'Neill, Paper presented at Miller-Combustion Engineering-Phosphazene Chemistry Workshop, U.S. Naval Academy, Annapolis, MD (1985).
19. R. M. Wightman, *Anal. Chem.*, **53,** 1125A (1981).
20. a, D. A. Buttry and F. C. Anson, *J. Am. Chem. Soc.*, **105,** 685 (1983); b, H. S. White, J. Leddy, and A. J. Bard, *ibid.*, **104,** 4811 (1982).
21. a, J. C. Jeager and M. Clarke, *Proc. R. Soc. Edinburgh,* **A61,** 229 (1942); b, M. Morita, M. Longmire, and R. W. Murray, Submitted to *Anal. Chem.*
22. C. D. Robitaille and D. Fauteux, *This Journal,* **133,** 315 (1986).
23. a, A. J. Bard and L. F. Faulkner, "Electrochemical Methods," p. 218, John Wiley & Sons, Inc., New York (1980); b, *ibid.*, p. 143.

Electrochemical Properties of Organic Disulfide/Thiolate Redox Couples

Meilin Liu, Steven J. Visco,* and Lutgard C. De Jonghe

Department of Materials Science and Mineral Engineering, University of California, and Materials and Chemical Sciences Division, Lawrence Berkeley Laboratory, Berkeley, California 94720

ABSTRACT

The redox behavior, kinetic reversibility, chemical reversibility and stability, and the specific adsorption or chemisorption at electrode surfaces of a diverse group of organodisulfide cathode materials have been studied by potential-sweep and potential-step methods. The number of electrons involved in the redox reaction and the diffusion coefficients of the organodisulfide species in electrolyte solutions were determined with a rotating disk electrode in conjunction with chronocoulometry/chronoamperometry. Observations indicated that the overall, stoichiometric reaction of these redox couples is

$$RSSR + 2e^- \rightleftarrows 2(RS^-)$$

where R represents an organic moiety. These reactions are chemically reversible, yet kinetically hindered, especially at ambient temperatures. The microscopic reversibility of the redox couples promises the possibility of constructing secondary energy conversion systems based on these materials. The slow electrode kinetics, however, indicates that the introduction of electrocatalysts to assist the electrode reaction may be effective in improving battery performance. The negligible adsorption of these materials at platinum electrodes, in addition, implies that the electrode kinetics can be formulated by simple electrodic equations without consideration of surface coverage.

A group of organic disulfides have been recently introduced as positive electrodes for high energy-density battery applications (1). The attractive features of these compounds include low operating temperatures (ambient to 150°C), high energy densities, low cost, passive behavior to many materials, and low toxicity. Furthermore, properties of the organodisulfides can be modified by appropriate choice of the organic groups. To date, however, the fundamental physical, chemical, and electrochemical properties of these materials have not been established. The purpose of this study has been to investigate the redox behavior, chemical stability/reversibility, kinetic reversibility, and adsorption phenomena of organodisulfides at electrode surfaces. The detailed analysis of electrode kinetics, reaction mechanism, electrocatalysis, and transport properties will be discussed in subsequent communications (18).

Experimental

A number of organic disulfides, sodium thiolate salts, and precursors were obtained from Aldrich Chemical Company, Incorporated, Milwaukee, Wisconsin 53233. Tetramethylthiuram disulfide (TMTD), tetraethylthiuram disulfide (TETD), and phenyl disulfide (PDS) were recrystallized several times from the appropriate alcohols (n-butanol, ethanol, etc.). Sodium diethyl dithiocarbamate (NaDEDC) and sodium dimethyl dithiocarbamate (NaDMDC) were purified by dissolving the salts in a minimum amount of absolute ethanol and precipitated by addition of absolute ether. The purified solid organosulfur compounds were stored under vacuum in a desiccator. Hydroxyethyl disulfide (HEDS) was distilled under vacuum over molecular sieves. Di-fluorophenyl disulfide (FPDS) was synthesized from the stoichiometric oxidation of 4-fluorothiophenol by iodine, and subsequently distilled under vacuum. Supporting electrolyte tetraethylammonium perchlorate (TEAP) and reference electrode filling electrolyte tetramethylammonium chloride (TMAC) were obtained from Southwestern Analytical Chemicals (Austin, Texas 78767) ground to fine powders, dried in a vacuum furnace at 80°C, and kept under vacuum in a desiccator. Anhydrous dimethylsulfoxide (DMSO) was

*Electrochemical Society Active Member.

obtained from Aldrich and stored over molecular sieves in an argon atmosphere dry box. Unless otherwise stated, all electrolyte solutions consisted of 0.1*M* TEAP in DMSO at 293 K. The electrolyte solutions were purged with dry argon for 10 min before each experiment.

Three-electrode electroanalytical cells with platinum auxiliary electrodes and Ag/AgCl reference electrodes (0.1*M* TMAC) were used throughout the experiments. Platinum metal, graphite, or glassy carbon planar electrodes were used as working electrodes. All working electrodes were polished to a mirror finish with diamond paste (1 μm) and rinsed with acetone before each experiment.

In potential sweep experiments (2-5), a linear or triangular potential function, generated using a PAR 173 potentiostat/galvanostat (PAR, Hayward, California 94545) in conjunction with a PAR 175 universal programmer, was applied to a stationary electrode immersed in a quiet solution. The corresponding currents were measured as a function of potential or time and recorded with a 4120T Bascom-Turner digital recorder (Bascom-Turner, Incorporated, Norwood, Massachusetts 02602). The sweep rates ranged from 1 to 1000 mV/sec.

In potential-step experiments (2, 3, 6-8), excitation signals of one or more potential steps (pulse width of 10-500 ms), were generated under computer control. Experiment control/data acquisition was accomplished by interfacing an IBM-PC/AT with a DT2801 data acquisition board (Data Translation, Incorporated, Marlborough, Massachusetts 01752) to a PAR 173 potentiostat/galvanostat by means of a program written in ASYST (Macmillan Software Company) language. Computer controlled output signals were applied to a stationary electrode immersed in a quiet solution and the corresponding current or charge responses were measured as a function of time. The potential of a working electrode (*vs.* Ag/AgCl) was stepped from an initial value, E_i, at which the system was at equilibrium (no apparent faradaic process), to a potential value at which the surface concentration of the electroactive species was effectively zero, ensuring diffusion control at all times. In the double potential-step methods, a square wave voltage function was used to step the interfacial potential from an initial value E_i to a potential, E_f, at which the forward reaction was completely controlled by diffusion, and then to a potential, E_r, at which the reverse reaction was completely controlled by diffusion. The potentials E_f and E_r were determined from chronoamperometric waves (2).

In rotating disk electrode (RDE) experiments (2, 3, 15-17), an ASR Electrode Rotator and Speed Controller (Pine Instrument Company, Grove City, Pennsylvania 16127) were used to modulate the rotation speeds of platinum or carbon working electrodes. Solution viscosities were measured using an Ostwald Viscometer. The convective-diffusion controlled currents were measured as a function of rotation speed.

Electrochemical Methods

Linear sweep voltammetry (LSV) and cyclic voltammetry (CV) have been used to characterize the redox behavior and the kinetic reversibility of the organodisulfide compounds (2-5). The determination of kinetic reversibility from experimental observations is important since it influences further interpretation of the experimental data. In electrochemical systems, a chemically stable redox couple is considered kinetically reversible if electron transfer is sufficiently rapid that the Nernst equation is always applicable, and voltammetric peak potentials (E_{pa} or E_{pc}) are independent of scan rate. For a kinetically irreversible process, however, the peak potentials depend on sweep rate (2).

The dependence of the peak currents and the peak potentials on sweep rate, the relationship between the peak currents and the peak potentials, and the separation of anodic and cathodic peak potentials in CV have been determined and used to characterize the redox behavior and to classify the systems studied in terms of kinetic reversibility.

Chronamperometry and chronocoulometry (2, 3, 6-8) have been used to study the chemical stability/reversibility of the redox couples and the adsorption of organodisulfide species at electrode surfaces (9-14). Under semi-infinite conditions (the solution sufficiently distant from the electrode surface is unperturbed), the diffusion-controlled components of chronoamperometric responses for the forward and reverse reactions at a planar electrode can be expressed as

$$i_f(t \leq \tau) = \frac{(n\mathbf{F}A)D_i^{1/2}C^*_i}{\pi^{1/2}}\frac{1}{t^{1/2}} \quad [1]$$

and

$$-i_r(t > \tau) = \frac{(n\mathbf{F}A)D_i^{1/2}C^*_i}{\pi^{1/2}}\left[\frac{1}{(t-\tau)^{1/2}} - \frac{1}{t^{1/2}}\right] \quad [2]$$

Under the assumption that the reactant (RSSR) is weakly adsorbed and the adsorption of the product (RS^-) is negligible, the chronocoulometric response in the forward direction can be expressed as

$$Q_f(t \leq \tau) = Q_{dl} + Q_d\,(t \leq \tau) + Q_{ads} \quad [3]$$

and the charge removed in the reverse direction can be expressed as

$$Q_r(t > \tau) = \frac{2(n\mathbf{F}A)D_i^{1/2}C^*_i}{\pi^{1/2}}[\tau^{1/2} + (t-\tau)^{1/2} - t^{1/2}] + Q_{dl} \quad [4]$$

where Q_{dl} is the charge due to double layer charging and Q_{ads} is the charge due to the reduction of the organodisulfide species adsorbed at electrode surface and is given by

$$Q_{ads} = n\mathbf{F}A\,\Gamma_i \quad [5]$$

The cumulative charge due to electrolysis of the electroactive species in the solution at a diffusion-controlled rate in the forward and reverse direction can be expressed as

$$Q_d(t \leq \tau) = \frac{2(n\mathbf{F}A)D_i^{1/2}C^*_i}{\pi^{1/2}}t^{1/2} \quad [6]$$

and

$$Q_d(t > \tau) = \frac{2(n\mathbf{F}A)D_i^{1/2}C^*_i}{\pi^{1/2}}[t^{1/2} - (t-\tau)^{1/2}] \quad [7]$$

In conjunction with single-step chronoamperometry and chronocoulometry, rotating disk electrode techniques were used to determine n, the number of electrons participating in the overall electrochemical reaction, as well as the diffusion coefficient of the organodisulfide species in electrolyte solutions (2, 3, 15-17). Under mass-transfer controlled conditions, the convective-diffusion limited current at a rotating disk electrode is given by

$$i_d(\omega) = 0.62\,(n\mathbf{F}A)C^*_iD_i^{2/3}\nu^{-1/6}\omega^{1/2} \quad [8]$$

where ν is the kinematic viscosity (cm^2/s) of the electrolyte solution and ω is the electrode rotation speed (Hz).

Results and Discussions

Redox behavior and kinetic reversibility.—Cyclic voltammograms of a group of organic disulfides on platinum electrodes in DMSO containing 0.1*M* TEAP are shown in Fig. 1. These voltammograms allow qualitative assessment of the kinetic (thermodynamic) reversibility of the redox couples. The most striking observation was the separation of the anodic and the cathodic peak potentials, which range from 1250 mV for TMTD at sweep rate of 20 mV/s, to 1630 mV for PDS at sweep rate of 100 mV/s. The large peak separations imply slow electrode reaction rates; the redox couples are kinetically irreversible at the sweep rates studied. Further, comparison of the separation of the peak potentials for different disulfides indicates the relative reversibility of the redox couples. At a given sweep rate, the smaller the peak separation the faster the electrode kinetics. Thus, for example, the redox couple TMTD/$DMDC^-$ is more reversible than the redox couple TETD/$DEDC^-$, and

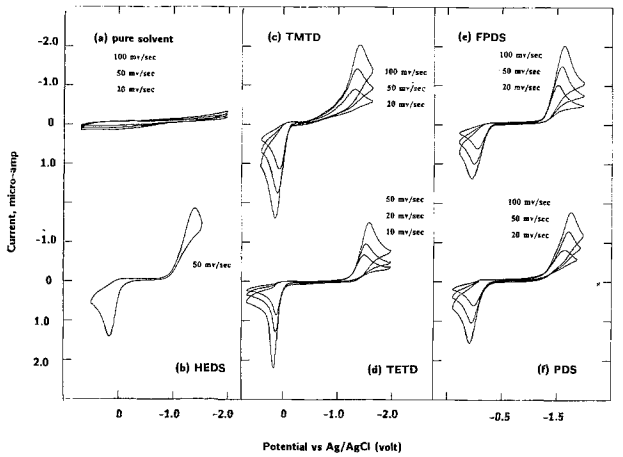

Fig. 1. Cyclic voltammograms of a group of organosulfur compounds in DMSO containing 0.1M TEAP at 293 K. (a) blank electrolyte solution; (b) 4.5 mM hydroxyethyl disulfide (HEDS), (HO-CH_2-CH_2-S-)$_2$; (c) 4.4 mM tetramethylthiuram disulfide (TMTD), [$(CH_3)_2$NCSS-]$_2$; (d) 4.2 mM tetraethylthiuram disulfide (TETD), ($(C_2H_5)_2$NCSS-)$_2$; (e) 4.1 mM di-fluorophenyl disulfide (FPDS), (F-C_6H_4-S-)$_2$; and (f) 3.6 mM phenyl disulfide (PDS), (C_6H_5-S-)$_2$. A microplatinum electrode (surface area = 4.1×10^{-3} cm^2) was used as working electrode and referenced to a Ag/AgCl electrode with a Luggin capillary salt bridge. The initial scan directions are reducing.

FPDS/FPT$^-$ is more reversible than PDS/PT$^-$. Kinetic reversibility, of course, is an important parameter for energy storage applications; the higher the kinetic reversibility of the electrode reaction, the higher the power output at a given energy efficiency of the system, or the higher the energy efficiency at a given power output. The slow kinetics of these redox couples calls for further investigation of electrode kinetics and electrocatalysis.

Cyclic voltammograms of TETD on different electrode materials are shown in Fig. 2. At identical scan rates, the peak potentials for TETD/DEDC$^-$ on graphite or glassy carbon electrodes were shifted in the positive direction with respect to platinum electrodes. This might be due to stronger adsorption of products or intermediate species at graphite electrodes, however, this issue needs further study. The observation of the dramatic positive displacement of cathodic peak potentials (247 mV), as opposed to the slight shift of the anodic peak potentials (23 mV), suggests that the anodic transfer coefficient is much greater

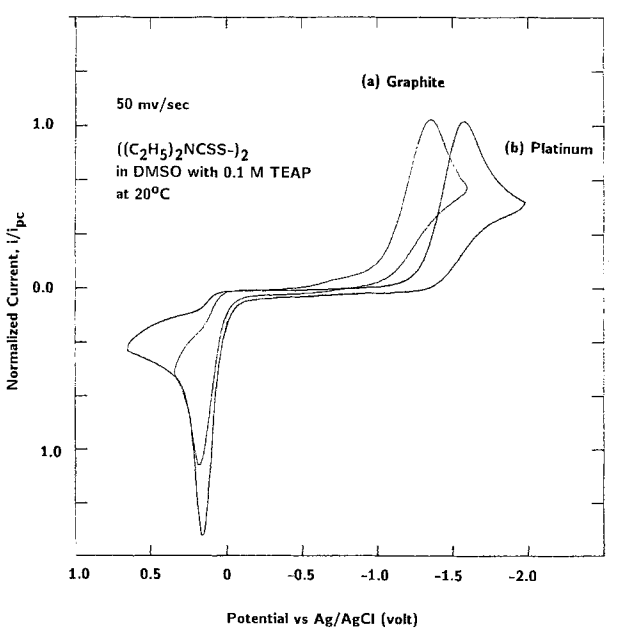

Fig. 2. Cyclic voltammograms of TETD on platinum and graphite electrodes in DMSO containing 0.1M TEAP at 293 K. The initial scan directions are reducing.

than the cathodic transfer coefficient. Also, the smaller separation of anodic and cathodic peak potentials on graphite electrodes relative to platinum electrodes indicates that the overall reaction rate is faster on graphite than on platinum. This was supported by rate constant measurements on different electrode materials (18). The study of kinetic reversibility at different electrode materials provides the basis for selection of electrode materials for battery applications. In fact, graphite felt has been used in our laboratory as a positive electrode current collector matrix for sodium and lithium batteries based on RSSR compounds.

The amplitudes of the peak currents (i_p) and the positions of the peak potentials (E_p) at different sweep rates were precisely determined from linear sweep voltammograms and from the corresponding differential voltammograms, as shown in Fig. 3 for reduction of TMTD to the thiolate anion DMDC$^-$. Similar voltammograms for the reverse process, *i.e.*, the oxidation of DMDC$^-$ to TMTD, are shown in Fig. 4. The analysis of i_p and E_p in both anodic and cathodic directions at different scan rates indicates that the relationships between i_p and $v^{1/2}$, between E_p and $\ln(i_p)$, and between $\ln(v)$ and E_p are approximately linear. Slight deviations at low sweep rates were probably brought about by non-planar diffusion. The linear relationship between these quantities further confirms that the redox couples are kinetically hindered and the introduction of appropriate electrocatalysts would be beneficial in an energy conversion device based on these organodisulfides.

In addition, the slopes of the linear plots, E_p *vs.* $\ln(i_p)$ and $\ln(v)$ *vs.* E_p, allow estimation of anodic and cathodic trans-

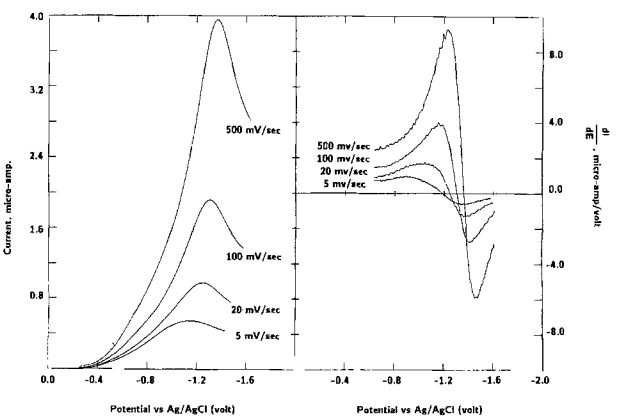

Fig. 3. Linear sweep voltammogram and the corresponding differential voltammogram for the reduction of TMTD to the thiolate anions DMDC$^-$ on a microplatinum electrode (surface area = 4.1×10^{-3} cm^2) at 293 K. Electrolyte solution: 4.4 mM TMTD in DMSO containing 0.1M TEAP.

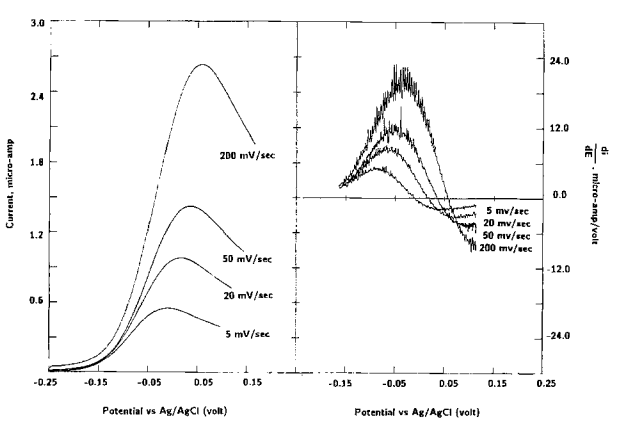

Fig. 4. Linear sweep voltammograms and the corresponding differential voltammograms for the oxidation of the thiolate anions DMDC$^-$ to the disulfide TMTD at a microplatinum electrode (surface area = 4.1×10^{-3} cm^2) at 293 K. Electrolyte solution: 8.1 mM NaDMDC in DMSO containing 0.1M TEAP.

fer coefficients, α_a and α_c. These parameters (18, 19) are as defined in the Butler-Volmer equation $[i = i_o \{\exp(\alpha_a \mathbf{F}\eta/RT) - \exp(-\alpha_c \mathbf{F}\eta/RT)\}]$. The plot of $\ln(i_p)$ *vs.* E_p at different sweep rates gives slopes of $-\alpha_c \mathbf{F}/RT$ for cathodic processes and $\alpha_a \mathbf{F}/RT$ for anodic processes. Similarly, the plot of E_p *vs.* $\ln(v)$ gives the slopes of $-RT/2\alpha_c \mathbf{F}$ and $RT/2\alpha_a \mathbf{F}$ for the cathodic and anodic processes, respectively. The transfer coefficients calculated from the observed data for TMTD/DMDC$^-$ are $\alpha_a = 0.62$ and $\alpha_c = 0.36$, obtained from $d\{\ln i_p\}/d\{E_p\}$, and $\alpha_a = 0.63$ and $\alpha_c = 0.37$, obtained from $d\{E_p\}/d\{\ln v\}$, and are in reasonable agreement with each other. Further, the summation of the observed anodic and cathodic transfer coefficients being equal to one indicates that the number of electrons transferred in the rate-determining step is equal to one.

Adsorption on electrode surface.—The absence of prepeaks and postpeaks in cyclic voltammograms implies that neither the reactants (RSSR) nor the products (RS^-) are strongly adsorbed at platinum electrodes. Further, there was no evidence that the thiolate anions (products) were weakly adsorbed. It is well known that if the product of reduction is weakly adsorbed, as potential sweep rate increases there is an anomolous positive shift of cathodic peak potentials with slight decrease of peak current, while anodic peak currents are enhanced (2). None of these phenomena were observed in the potential sweep experiments at platinum electrodes. This is also supported by the chronocoulometric measurements as shown in Fig. 6, where the intercepts in the reverse direction for organodisulfide solutions nearly overlap with the intercept (Q_{dl}) for blank electrolyte solution.

The total cumulative charge, Q, acquired by a computer in double-step chronocoulometry is shown in Fig. 5. Curve (x) represents the charge contribution from the blank electrolyte solution (0.1*M* TEAP in DMSO), and is mainly due to the charging of the double layer at electrode surface. The featureless appearance of this curve indicates that the solvent (DMSO) and the supporting electrolyte (TEAP) are sufficiently stable at the potentials applied. The other curves represent the total charge response of various organic disulfide species in the electrolyte solution. The total charge response is actually the sum of the charges due to (*i*) the electrolysis of the electroactive species at diffusion-controlled rate, Q_d, (*ii*) the double layer charging, Q_{dl}, and (*iii*) the electrolysis of the adsorbed electroactive species at the electrode surface, Q_{ads}.

The linear plots of the cumulative charge $Q_f(t < \tau)$ *vs.* $t^{1/2}$ and the charge removed in the reverse direction $Q_r(t > \tau)$ *vs.* $[\tau^{1/2} + (t - \tau)^{1/2} - t^{1/2}]$ are shown in Fig. 6. The intercept in

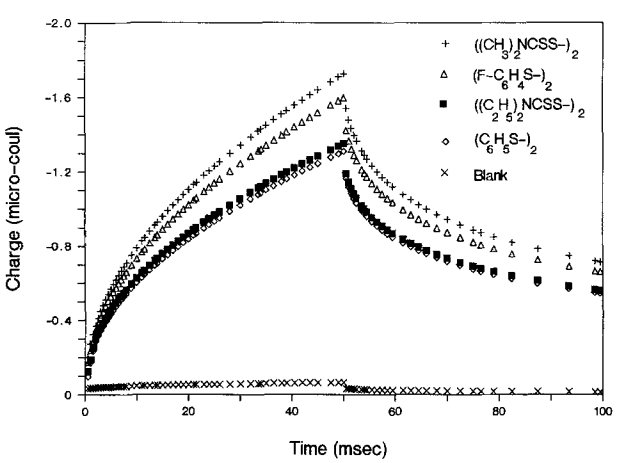

Fig. 5. Chronocoulometric response of a group of organic disulfides in DMSO containing 0.1M TEAP. (×) Blank electrolyte solution, (+) 4.4 mM tetramethylthiuram disulfide, (■) 4.1 mM tetraethylthiuram disulfide, (△) 4.1 mM di-fluorophenyl disulfide, and (◇) 3.7 mM phenyl disulfide. The surface area of the microplatinum working electrode is 4.1×10^{-3} cm^2. Potentials (*vs.* Ag/AgCl) were stepped from the rest potential (−0.25V) to cathodic active potential −2.1V for reduction, then to anodic active potential +0.4V for oxidation, and finally back to the rest potential. The duration of the potential steps was 50 ms.

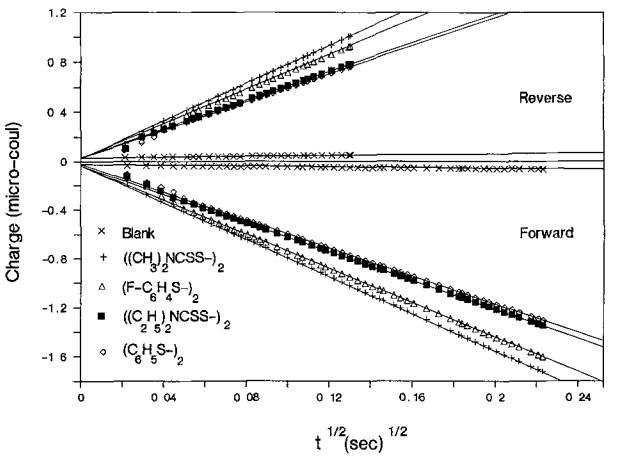

Fig. 6. Linear plot of the chronocoulometric response data shown in Fig. 5. The plot of the total charge in the forward direction $Q_f(t < \tau)$ *vs.* $t^{1/2}$ gives intercepts of $[Q_{dl} + Q_{ads}]$. The plot of the charge removed in the reverse direction $Q_r(t > \tau)$ *vs.* $[\tau^{1/2} + (t - \tau)^{1/2} - t^{1/2}]$ gives the intercepts of Q_{dl}. The difference between the two intercepts gives the charges due to adsorption of electroactive species at electrode surface, $Q_{ads} = n\mathbf{F}A\Gamma_i$. The slope in either direction is S_1, as defined by Eq. [9].

the forward direction is the sum of Q_{dl} and Q_{ads}, and in the reverse direction is Q_{dl}. The difference between the two intercepts directly gives the charge due to adsorption of electroactive species at electrode surface, $Q_{ads} = n\mathbf{F}A\Gamma_i$. The intercepts in both directions, and the charges due to adsorption are tabulated in Table I for different disulfides. The results indicate that the adsorption of these species on platinum electrode is negligible. Further, as it is evident from Eq. [3] and [4], the slopes of the linear plots in both directions can be expressed as

$$S_1 = \frac{2(n\mathbf{F}A_1)D_i^{1/2}C^*_{i,1}}{\pi^{1/2}} \qquad [9]$$

where A_1 is the effective surface area of the microworking electrode, $C^*_{i,1}$ is the bulk concentration of the electroactive species i in the chronocoulometric experiment, and the other notations have the standard meanings. These slopes will be used later to estimate the number of electrons involved in the overall reaction and the diffusion coefficients of the organodisulfide species in the electrolyte solution.

Chemical stability and reversibility.—The ratio of the diffusion-controlled currents from chronoamperometric response and the ratio of diffusion-controlled charges from chronocoulometric response are characteristics of the chemical stability/reversibility of a redox couple. The ratios of $-i_r(2\tau)/i_f(\tau) = 0.2929$ and $Q_d(2\tau)/Q_d(\tau) = 0.4142$ imply the system studied is chemically stable and reversible. Deviations from these ratios, however, indicate chemical complications. The ratios calculated from observed data for different disulfides are listed in Table II. The experimental values closely match the theoretical values indicating that the system is chemically stable and reversible under the present experimental conditions. In other words, both the oxidized and reduced forms are chemically stable and reversible, so that the reaction can be carried out in either direction. This microscopic reversibility

Table I. Adsorption of organodisulfide species at platinum electrode at 293 K (determined from chronocoulometry)

Organic disulfide	$C^*_{i,1}$ [m*M*]	$Q_{dl} + Q_{ads}$ [μC]	Q_{dl} [μC]	$Q_{ads}n$ [μC]	$\mathbf{F}\Gamma_i$ [μC/cm^2]
TMTD	4.4	0.0323	0.0256	0.0067	1.63
TETD	4.1	0.0361	0.0314	0.0047	1.15
FPDS	4.1	0.0342	0.0277	0.0065	1.59
PDS	3.7	0.0302	0.0272	0.0030	0.732

Table II. The ratios of diffusion-controlled currents and the ratios of diffusion-controlled charges obtained from the potential-step experiments at 293 K

Organodisulfide	$\frac{-i_r(2\tau)}{i_f(\tau)}$	$\frac{Q_d(2\tau)}{Q_d(\tau)}$
TMTD	0.2940	0.4121
TETD	0.2995	0.4140
FPDS	0.2996	0.4137
PDS	0.2987	0.4149

is a fundamental criterion for secondary energy storage systems.

Number of electrons involved in the overall reactions and diffusion coefficients.—The convective-diffusion limited current at an RDE (Eq. [8]), $i_d(\omega)$, *vs.* $\omega^{1/2}$, *i.e.*, the Levich plot, is shown in Fig. 7 for the reduction of a group of organic disulfides on graphite electrodes in DMSO containing 0.1*M* TEAP. The viscosities of various electrolyte solutions used in the RDE studies were determined using an Ostwald viscometer and are listed in Table III. The slopes [$\mu A\ s^{1/2}$] of the Levich plots can be expressed as

$$S_2 = 0.62\,(n\mathbf{F}A_2)C^*_{i,2}D_i^{2/3}\nu^{-1/6} \qquad [10]$$

where A_2 is the effective surface area of the rotating disk electrode and $C^*_{i,2}$ is the bulk concentration of the electroactive species i in the RDE experiment.

Linear plots of chronoamperometric responses for reduction of different disulfides at platinum electrodes in DMSO are shown in Fig. 8. The slight deviation from strict linearity, particularly after the potential was stepped from the rest potential to the active cathodic potential, was probably due to double layer charging. The slopes of these plots can be expressed as

$$S_3 = S_1/2 \qquad [11]$$

From these slopes, the number of electrons involved in the overall reaction can be calculated as

$$n = 0.1470\,\frac{1}{\mathbf{F}\nu^{1/2}}\,\frac{S_1^4}{S_2^3}\,\frac{(A_2C^*_{i,2})^3}{(A_1C^*_{i,1})^4} \qquad [12]$$

and the diffusion coefficient can be estimated as

$$D_i = 36.3396\nu\left(\frac{S_2}{S_1}\,\frac{A_1C^*_{i,1}}{A_2C^*_{i,2}}\right)^6 \qquad [13]$$

The slopes of these plots, S_1, S_3, and S_2, the diffusion coefficients, D_i, and the number of electrons participating the overall reaction, n, for various organosulfur compounds are tabulated in Table III.

Since the calculated number of electrons involved in the reduction of these organic disulfides are reasonably close to 2.0 (within experimental error), the overall, stoichiometric reaction takes the form of

$$RSSR + 2e^- \rightleftharpoons 2(RS^-) \qquad [14]$$

where R represents an organic moiety. Furthermore, the observation of two electrons involved in the overall reaction and one electron transferred in the rate-determining step suggests that the electrode reaction is a multi-step two-electron transfer reaction. The detailed reaction mechanism will be discussed in a subsequent communication (18).

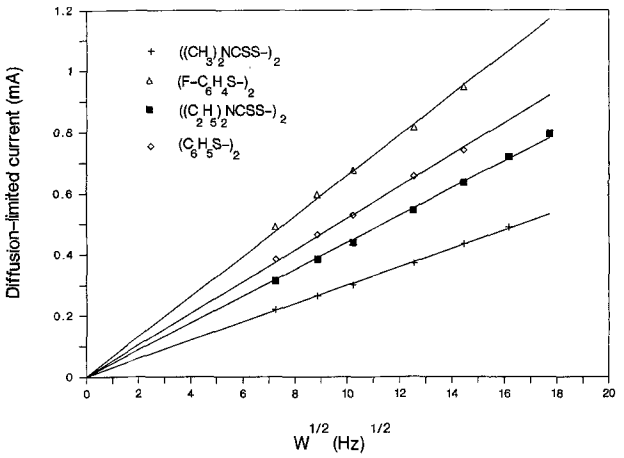

Fig. 7. Levich plots for the reduction of a group of organic disulfides in DMSO containing 0.1M TEAP. (+) 1.1 mM tetramethylthiuram disulfide, (■) 2.1 mM tetraethylthiuram disulfide, (△) 2.5 mM di-fluorophenyl disulfide, and (◇) 2.2 mM phenyl disulfide. Potential (vs. Ag/AgCl) sweep rate was 10 mV/s. Rotation speed ranged from 500-3000 rpm. Surface area of the working electrode was 0.50 cm^2.

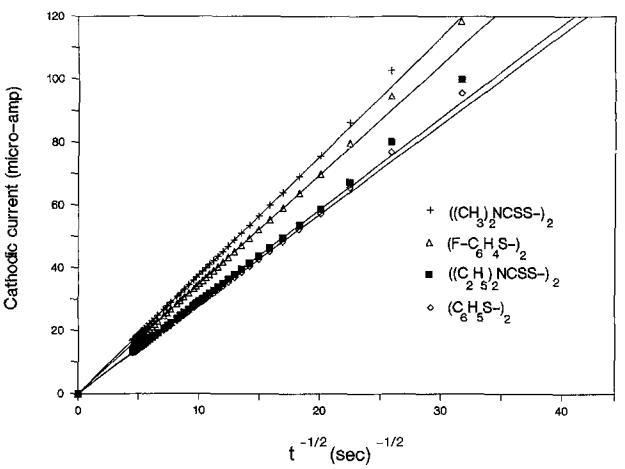

Fig. 8. Linear chronoamperometric plots in single-step chronoamperometry. (+) 4.4 mM tetramethylthiuram disulfide, (■) 4.1 mM tetraethylthiuram disulfide, (△) 4.1 mM di-fluorophenyl disulfide, and (◇) 3.7 mM phenyl disulfide. Microplatinum electrode surface area was 4.1×10^{-3} cm^2. Potentials (vs. Ag/AgCl) were stepped from the rest potential (−0.25V) to active potential (−2.1V) for reduction, and then back to the rest potential. The duration of the potential steps was 50 ms.

Conclusions

The organodisulfide/thiolate redox couples, $RSSR/RS^-$, are chemically reversible yet kinetically slow. The overall stoichiometric reaction for these redox couples is described by Eq. [14], which must involve multistep elementary reactions. The microscopic reversibility of these processes, in principle, makes it possible to construct rechargeable batteries based on the organic disulfides. The

Table III. The number of electrons transferred in the electrode reaction and the diffusion coefficient of the organodisulfide species in DMSO containing 0.1M TEAP at 293 K (determined from RDE in conjunction with chronocoulometry/chronoamperometry)

Organic disulfide	$C^*_{i,1}$ (m*M*)	S_1 $\left(\frac{\mu C}{s^{1/2}}\right)$	S_3 $\left(\frac{\mu A}{s^{1/2}}\right)$	$C^*_{i,2}$ (m*M*)	ν $\left(\frac{cm^2}{s}\right)$	S_2 $\left(\frac{\mu A}{Hz^{1/2}}\right)$	RDE + chronocoulometry n	RDE + chronocoulometry $D_i \times 10^6$ $\left(\frac{cm^2}{s}\right)$	RDE + chronoamperometry n	RDE + chronoamperometry $D_i \times 10^6$ $\left(\frac{cm^2}{s}\right)$
TMTD	4.4	7.54	3.76	1.1	0.021655	29.5	2.0475	3.51	2.0259	3.57
FPDS	4.1	6.95	3.47	2.5	0.021101	65.9	2.0914	3.29	2.0794	3.32
PDS	3.7	5.75	2.86	2.2	0.022143	51.8	2.0237	2.96	1.9818	3.04
TETD	4.1	5.86	2.94	2.1	0.021799	44.7	1.9751	2.62	2.0022	2.57

relatively slow electrode kinetics indicate that the introduction of suitable electrocatalysts will probably prove useful. Since the adsorption of organic disulfides on platinum electrodes is negligible the electrode kinetics can be described using simple electrodic equations, and studied without consideration of surface coverage.

Acknowledgment

This work was supported by the Assistant Secretary for Conservation and Renewable Energy, Office of Energy Storage and Distribution, Energy Storage Division of the U.S. Department of Energy under Contract no. DE-AC03-76SF00098.

Manuscript submitted July 29, 1988; revised manuscript received Jan. 17, 1989.

Lawrence Berkeley Laboratory assisted in meeting the publication costs of this article.

LIST OF SYMBOLS

A	surface area of an electrode (cm^2)
A_1	surface area of the microplatinum electrode, $A_1 = 4.1 \times 10^{-3}$ (cm^2)
A_2	surface area of the rotating disk electrode, $A_2 = 0.50$ cm^2
C^*_i	bulk concentration of species i (μmol cm^{-3})
$C^*_{i,1}$	bulk concentration of species i in potential-step experiment (μmol cm^{-3})
$C^*_{i,2}$	bulk concentration of species i in RDE experiment (μmol cm^{-3})
D_i	diffusion coefficient of species i (cm^2 s^{-1})
E_i	initial potential (V)
E_f	potential of working electrode during forward step (V)
E_p	peak potential in voltammetry (V)
E_{pa}	anodic peak potential in voltammetry (V)
E_{pc}	cathodic peak potential in voltammetry (V)
E_r	potential of working electrode during reverse step (V)
F	Faraday's constant, 96,487 (C equiv.$^{-1}$)
i_d	diffusion-limited current or convective-diffusion limited current (μA)
i_f	current due to diffusion-controlled electrolysis during forward step (μA)
i_p	peak current in voltammetry (μA)
i_{pa}	anodic peak current in voltammetry (μA)
i_{pc}	cathodic peak current in voltammetry (μA)
i_r	current due to diffusion-controlled electrolysis during reverse step (μA)
n	number of electrons transferred in the overall reaction
Q	total charge (μC)
Q_{ads}	charge due to electrolysis of adsorbed species (μC)
Q_d	cumulative charge due to electrolysis of electroactive species at diffusion-controlled rate (μC)
Q_{dl}	charge due to double layer charging (μC)
Q_f	total cumulative charge during forward step (μC)
Q_r	total charge removed during reverse step (μC)
R	universal gas constant, $R = 8.3143$ (J mol^{-1} K^{-1})
S_1	slope of linear chronocoulometric plot (μC $s^{-1/2}$)
S_2	slope of Levich plot (μA $s^{1/2}$)
S_3	slope of linear chronoamperometric plot (μA $s^{1/2}$)
t	time (s)
T	absolute temperature (K)
v	potential sweep rate (mV s^{-1})
α_a	anodic transfer coefficient
α_c	cathodic transfer coefficient
β	symmetry factor
T_i	surface concentration of adsorbed species i (μmol cm^{-2})
ν	kinematic viscosity of an electrolyte solution (cm^2 s^{-1})
τ	characteristic pulse width (s)
ω	rotation speed of disk working electrode (Hz)

Subscripts

a	anodic
c	cathodic
f	forward direction
p	peak
r	reverse direction

Abbreviations

CV	cyclic voltammetry
$DEDC^-$	diethyl dithiocarbamate anion, $[(C_2H_5)_2NCSS]^-$
$DMDC^-$	dimethyl dithiocarbamate anion, $[(CH_3)_2NCSS]^-$
DMSO	dimethylsulfoxide, CH_3SO
HEDS	hydroxyethyl disulfide, $(HO\text{-}CH_2\text{-}CH_2\text{-}S\text{-})_2$
FPDS	di-fluorophenyl disulfide, $(F\text{-}C_6H_4\text{-}S\text{-})_2$
FPT^-	fluorophenyl thiolate anion, $[F\text{-}C_6H_4\text{-}S]^-$
LSV	linear sweep voltammetry
NaDEDC	sodium diethyl dithiocarbamate, $(C_2H_5)_2NCSS\text{-}Na$
NaDMDC	sodium dimethyl dithiocarbamate, $(CH_3)_2NCSS\text{-}Na$
PDS	phenyl disulfide, $(C_6H_5\text{-}S\text{-})_2$
PT^-	phenyl thiolate anion, $[C_6H_5\text{-}S]^-$
RDE	rotating disk electrode
RS^-	a group of thiolate anions, R represents an organic moiety
RSSR	a group of organic disulfides, R represents an organic moiety
TEAP	tetraethylammonium perchlorate, $[(C_2H_5)_4\ NClO_4]$
TETD	tetraethylthiuram disulfide, $((C_2H_5)_2NCSS\text{-})_2$
TMAC	tetramethylammonium chloride, $(CH_3)_4NCl$
TMTD	tetramethylthiuram disulfide, $((CH_3)_2\ NCSS\text{-})_2$

REFERENCES

1. S. J. Visco, C. C. Mailhe, L. C. De Jonghe, and M. B. Armand, *This Journal*, **136,** 661 (1989).
2. A. J. Bard and L. R. Faulkner, "Electrochemical Methods, Fundamentals and Applications," Wiley, New York (1980).
3. W. R. Heineman and P. T. Kissinger, in "Laboratory Techniques in Electroanalytical Chemistry," p. 52, Marcell Dekker, Inc., New York (1984).
4. J. Heinze, *Angew. Chem. Int. Ed. Engl.*, **23,** 831 (1984).
5. V. D. Parker, in "Electroanalytical Chemistry," Vol. 14, pp. 1-111, Marcel Dekker, Inc., New York (1986).
6. H. J. Christie, R. A. Osteryoung, and F. C. Anson, *J. Electroanal. Chem.*, **13,** 236 (1967).
7. M. K. Hanafey, R. L. Scott, T. H. Ridgway, and C. N. Reilly, *Anal. Chem.*, **50,** 116 (1978).
8. F. C. Anson, *ibid.*, **38,** 54 (1966).
9. J. H. Christie, *J. Electroanal. Chem.*, **13,** 79 (1967).
10. T. H. Ridgway, R. P. Van Duyne, and C. N. Reilley, *ibid.*, **34,** 267 (1972).
11. K. Holub and J. Weber, *ibid.*, **73,** 129 (1976).
12. F. C. Anson and R. A. Osteryoung, *J. Chem. Educ.*, **60,** 293 (1983).
13. B. Case and F. C. Anson, *J. Phys. Chem.*, **71,** 402 (1967).
14. G. W. O'Dom and R. D. Murray, *Anal. Chem.*, **39,** 51 (1967).
15. V. Y. Filinovsky and Y. V. Pleskov, in "Comprehensive Treatise of Electrochemistry," Vol. 9, p. 293, Plenum Press, New York (1981).
16. J. S. Newman, "Electrochemical Systems," Prentice-Hall, Englewood Cliffs, NJ (1972).
17. R. W. Zurilla, R. K. Sen, and E. Yeager, *This Journal*, **125,** 1103 (1978).
18. M. Liu, S. J. Visco, and L. C. De Jonghe, *This Journal*, Accepted for publication.
19. J. O'M. Bockris and A. K. N. Reddy, "Modern Electrochemistry," Vol. 2, Plenum Press, New York (1970).